ICAS-88-3.10-3

# EXPERIENCE IN APPLICATION OF ACTIVE VIBRATION CONTROL TECHNOLOGY TO A WIND TUNNEL MODEL AND TO FLYING AIRBUS

Klaus Koenig
MBB-UT, P.O. Box 10 78 45, 2800 Bremen, Germany

## Abstract

Vibration control technology based on the modified optimal control theory has been applied to a wind tunnel model and to the flying Airbus. Analog and digital controllers, tuned observers and broad band controller laws, ailerons, spoilers and wing tip vanes, together with different sensor locations have been tested in calm and turbulent atmosphere as well as with and without failure modes.
Test results were promising and allowed larger increase of flutter speed as well as amplitude reduction together with load alleviation for the studied examples. Some know-how has been acquired.

## 1. Introduction

Vibration control is the subject of the studies to be reported on in the following. The work was sponsored by the German government and the author would first of all like to thank all his colleagues who contributed to the success of this work.

Vibration control means reduction of unwanted elastic deformations, most often with the aim of avoiding restricting flutter speeds and alleviating gust loads as much as possible.
Yet this modern technology is not a simple one. A larger number of parameters have an influence. Problems may arise where they were never expected and the final success may be largely dependent on the individual basic aircraft design.
For example, the aerodynamic control surfaces used may - but should not - impair the aircraft's rigid body stability, its maneuverability and its ride comfort.

Furthermore, it is obvious that powerful effects can only be achieved if powerful control surfaces are available from the beginning. A possible benefit would be endangered if it were necessary to install extra weight to have such surfaces available.

## 2. General Remarks about the Controller Design

In the following all design work is based on the well known optimal control theory (see reference (1)) which requires a linear mathematical model in time domain.

### 2.1 The Mathematical Model

Of course the mathematical model must represent each and every part contributing to the dynamic behaviour of the plant (this is the system to be controlled) and of the controller. Even known practical degradation or deviation from the ideal regulator law to be designed must be included, as for example the time delay due to the computation time in digital controllers or the difference between pseudo and ideal integration, if used.

The unsteady aerodynamics is of special interest. Most often it is available in frequency domain and is computed, for example, by the double lattice method. A transformation in time domain is necessary and this is often done by polynomial approximation with inclusion of so-called lag states (2). However, a good approximation requires some lag states and inflates the mathematical model as well as the computation costs. To avoid this, an alternative has been used which could be called modal synthesis. It does not use the aerodynamics directly. It starts from a classical flutter calculation where the aerodynamics has already been processed and assumes that the complex eigenvectors and eigenvalues found are all valid at the same time and that the airloads are not very much influenced by acceleration terms.
The complete dynamic equation may read as equation 2.1-1 in Fig. 2.1-1 where the pL are the aerodynamic loads and the pH are the additional (internal) actuator loads resulting from electrical control signals.
If one assumes for a while that equation 2.1-2 is valid, one can combine equation 2.1-1 and -2 resulting in equation 2.1-3.
An eigenvalue calculation yields equation 2.1-4 and with the neglection of ML in the pH term, equation 2.1-5 results from equation 2.1-3 and -4.
Equation 2.1-6 gives the abbreviation.
This is the classical state equation of a dynamic system. Its matrices can be immediately computed if MS is taken as the original mass matrix of the structural weight and if the eigenvalues $\lambda F$ and the eigenvectors $\Phi F$ are taken from any flutter calculation, be it as advanced as one likes.

A comparison is given later in connection with the Airbus tests. Yet the method of modal syntheses has always been used in the following.

### 2.2 Suboptimal Approximation of Controller

A special problem of application of the optimal control theory results from the fact that this theory is based on the feed back of signals from all states. Often this is simply not possible because some states are not measurable and even if possible this would involve higher expenses. But fortunately it is not necessary to know everything provided the most important things are known.
Fig 2.2-1 gives an example of a system with 6 states. Nyquest diagrams of transfer functions of the plant plus controller $H_{u_T u}(\omega)$ in an open loop condition are plotted. These are functions of regulator response due to an input signal into the actuator of the aircraft control surface.

Pure theory requires that signals of all 6 states are fed back. But the lower diagram shows how the transfer function changes if one adds to the regulator input one state signal after the other from No 1 up to No 6. It is obvious that not all states contribute to the same extent. Therefore it should be possible to neglect some of them as is shown in the upper diagram of Fig 2.2-1 where the optimal and the non-optimal transfer function with a reduced number of feed back signals are compared.
To compensate for the resulting differences partially it should further be possible to change the controller coefficients of the remaining states to get the best approximation of the optimal transfer function. For the following this has been done by minimising the sum of squared differences between the optimal and the "suboptimal" transfer function in the frequency range of interest.

A summary of the principles of suboptimal controller design is given in Fig. 2.2-2.

## 2.3 Observers

As another means of compensation for a reduced feed back observers are proposed. In addition to the usual controller coefficients of the optimal control theory some differential equations of the system are installed into the controller. This is done basically to substitute an unmeasured signal by a computed one.
The well known Kalman-Bucy filter (1) tries to compensate for all missing information while the observers proposed in (2) operate with a reduced order of the differential equations.
In the tests to be described in the following some observers of the latter type have been checked.
Fig. 2.3-1 shows the principle signal flow illustrating the complexity of the observer.

## 2.4 Roll-off Filters

If it is reasonable to concentrate on the important information only, then it was thought worthwile also to install an electrical bandpass filter additionally to roll-off all unwanted disturbances from the measured signals.
Electrical noise and high frequency structure response can thus be excluded by the low pass of the filter. Yet further it is also possible to decouple the low frequency rigid body movement from the vibrations to be controlled by the high pass of this filter.

## 2.5 Sensor Location

By location of sensors, geometric filtering is possible (antisymmetric or symmetric).
It should, however, also be tried to place the pick ups in such a way that each one measures just one of the relevant degrees of freedom strongly.
In this case the controller signal is built up as a sum of small values but not from a difference of large values. Figure 2.5-1 gives two examples for two suboptimal controllers of the same system with nearly the same open loop Nyquist diagram. But if one looks for the contribution of the individual feed back lines, the tremendous differences are evident.

## 2.6 Safety aspects

The application of artificial means for load alleviation or even flutter suppression poses the question of the safety or robustness against disturbances of such means.
Safety against disturbances from outside can be reached very simply if only linear control circuits are used and if the controller law guarantees sufficiently large damping values of all eigen vibrations of the complete system (plant + controller) in closed loop operation.

Internal disturbances may arise from different sources. However, for modern aircraft with „fly by wire" technology a special safety concept must be developed which copes with most of them. Therefore it may be sufficient in this context to look only at the disturbances of the sensor signals and at the available gain and p..ase margins of the complete system. The latter are measures of safety of the whole circuit of signal, controller and plant against smaller de.iations from theoretical design.
These margins can be read from the Nyquist diagram of plant with controller in open loop condition.

Yet unfortunately these margins are of restricted value as one can also see in Fig. 2.5-1.
Both controllers give about the same available margins but if one of their critical feed back lines fails the necessary margin to keep stability with the one controller will be very different from that with the other controller.
To cope with signal disturbances, a signal conditioner can be designed which should monitor and vote the redundant signals in such a way that failures are recognized and the transfered signal guarantees the best continuation of flight.
The principle signal flow in a possible signal conditioner for a pseudo quadruplex signal is shown in Fig. 2.6-1 as an example. (Details can not be given within the scope of this paper).

# 3. Applications to a Wind Tunnel Model

## 3.1 Model and Tunnel

The model was installed in the 3 m tunnel of DFVLR in Göttingen, Germany. It is a full flexible model with controllable ailerons, spoilers and taileron (or elevator). For details see (3).
The model showed two types of instability. The first was a small rigid body instability of heave and pitch movement. It appeared at about 30 kts wind speed with a frequency of about 0.5 Hz.

The second instability was a classical wing flutter case caused by coupling of wing bending and torsion. It appeared with about 6 Hz (torsion mode) at a wind velocity between 39 and 40 m/s depending on the campaign and the minor changes of the model put into effect in the meantime.

The installation of sensors used to measure vertical acceleration, pitch velocity and wing root moments during the tests is shown in Fig. 3.1-1.

## 3.2 The Controllers

A large number of controllers were tested. Fig.3.2-1 gives a survey of the most important ones. 3 controllers were applied to the taileron, 6 to the ailerons and 2 out of the 6 (but with doubled gain) to the spoilers. 4 of them were analog and 7 were digital. The 3 suboptimal controllers applied to the taileron were designed as pitch dampers to cure the rigid body instability. One of the others was designed to improve the flutter speed and reduce the wing bending moment at the same time and the others to increase the flutter speed as much as possible.

Butterworth filters as roll-off bandpasses were used, but no notch filters. Pseudo integration by a low pass of first order (T/(sT+1) with T= 2 sec) has always been used to build up the states of interest (deformation and velocity) from the measured signals (acceleration or velocity). Only for the controller (G4.2D), accelerations have been used as a direct feed back as described in (2).

Observers of reduced order were designed twice. They were of 4th order while the basic mathematical model was of 14th order. Input signals from only one pair of sensors were used for these controllers with observers.
Their transfer functions together with the transfer functions of the suboptimal controller without observer which they are based on are shown in Fig. 3.2-2.
These curves include the roll-off filters. One can see very clearly how the observer of reduced order produces a peak in magnitude which will make the controller very sensitive to changes of plant or aircraft model due to weight or flight velocity changes.
Further one can see the effect of pseudo integration very clearly.

## 3.3 Results

### 3.3.1 Flutter Speed

The wind velocities reached with the different controllers are given in Fig. 3.2-1.
The maximum value was more than 58 m/s (tunnel limit) to be compared with about 40 m/s found without controller. That is an increase by more than 45% of velocity or by 110% of dynamic pressure.

Reductions of this benefit are, however, possible:

- o By use of reduced order observer (57 to 53 m/s)
- o By direct use of signals from one side of the model instead of pairs from left and right side (56 to 55 m/s)
- o By a reduced input due to failures (one pair of signals instead of two pairs) (57 to 52 or 47 m/s)
- o By use of different sensor sets even if optimal control theory gives equal results (57 to 56 m/s)
- o By adding a load alleviation function (56 to 54 m/s)

No influence could be found within the scatter of the test results for:

- o The use of analog or digital controllers
- o The different approximations and inclusion of the roll-off filters

Moreover there were indications that the different taileron controllers used simultaneously with the aileron controllers also had some influence on the flutter speed.

### 3.3.2 Load Alleviation

Application of active control technologies for load alleviation is of major interest.
Therefore one regulator (G 2.3) was designed for flutter suppression and load alleviation at the same time.
This has been done by using different weighting matrices of the states (QX) during computation of controller coefficients and by selection of that controller which showed the largest amount of modal damping for the wing bending mode.

A result is shown in Fig. 3.3.2-1 where autospectra of the wing root bending moment with and without controllers are given.
Superimposed are artificial gusts with a scaled corner frequency of 5 Hz. The reduction reached by the controller is remarkable.

Fig. 3.3.2-2 shows the benefit for different velocities. It increases with velocity. Starting with 16% reduction at 20 m/s it reaches 37% at 35 m/s where the level of loads is even higher.

Fig.3.3.2-3 permits a comparison of the influence of the different controllers on the loads.

### 3.3.3 Safety Tests

To study this question several tests have been performed.
First, it could be shown that the stability of plant and controller or the characteristics of the controller are not changed by extraneous disturbances as to be expected for linear systems. Application of heavy harmonic gusts tuned to the frequency of flutter, or of superimposed signals (frequency sweep) at the aileron actuator signal input did not result in any problem. Stability of controller G 3.1A at a velocity of 57 m/s was unimpaired, of course with larger amplitudes of structural vibration, aileron movement and loads.

The influence of monitoring and voting has been studied with controller G 3.1A and for signal conditioning as shown in Fig. 2.6-1. One out of the four signals fed back was tripled, analog/digital converted, disturbed, conditioned, digital/analog converted and given back to the normal signal flow. The second signal belonging to the same sensor pair of symmetrically located sensors was undisturbed but digitized and made available in the signal conditioner while the remaining two other signals of the second sensor pair stayed unchanged and analog.
Fig. 3.3.3.-1 gives an example where signal B5 is disturbed. One line of this signal has already failed and another is disturbed by an arbitrarily increased harmonic signal with 6.3 Hz (about the flutter frequency).
If the amplitude becomes too large, that means if

the difference between the two remaining data is too big, the signal conditioner does not accept signals from B5 any longer and uses B15 (the symmetric equivalent) instead. In the figure it can be seen that this process is not an abrupt one. It is some time until sensor B5 is declared as failed completely. After that the remaining differences shown result from data processing (about 4 ms) and mainly from differences between signals from right and left side.
These latter differences were not so large for the model under investigation, allowing to proceed as shown. Nevertheless, it must be borne in mind that there was no frequency of an antisymmetric mode within the bandwidth of interest.

To study the effect of a control surface failure Fig. 3.3.3-2 shows how the model behaves if in overcritical flight condition the controller is switched off and switched on again. One can see how the amplitudes of vibration increase after switch off and how quickly they disappear again after switch on.
So if one control surface fails it should be possible to switch over to another one even in overcritical flight.
Fig. 3.3.3-3 gives an example at moderate conditions. Even with one second signal interruption no critical vibration is visible.

## 4. Application to Airbus

Another application of active control technology was possible during flight vibration testing of one of the wide body Airbus aircraft.

### 4.1 Aircraft and Tip Vane System

This aircraft had no outer aileron which could be used for vibration control. Therfore additional control surfaces at the tips of the wing (tip vanes) had been installed as a means of excitation during flight vibration testing (4). If these little surfaces (0.2% of wing area) were able to excite the aircraft for vibration they should also be able to control vibrations if there were any.

Fig.4.1-1 shows the aircraft and the locations of the sensors used for these tests.

Now it must be said that the original aircraft has of course but "unfortunately" no critical vibration. Therefore if vibration control technology was to be tested on this available aircraft something had to be changed.

After some studies it was found that by special mass or stiffness arrangements one of the vibration modes (engine vertical movement or pitch) could be influenced in such a way that its damping will start to decrease just at the maximum aircraft speed $V_D$. Fig. 4.1-2 shows the results of a flutter calculation for the modified aircraft. Everything stated below relates to this aircraft. From Fig. 4.1-2 one can see that wing bending mode (wb) and engine pitch mode (Ez) are coupling. That leads to the dip in the curve of damping of engine pitch mode.
It was the aim of the study to cure this dip or to change the modal damping of engine z mode.

### 4.2 The Controllers

Three different controllers were tested. They were named A 1.3; A 1.4 and A 2.8.
All used the same symmetric sensor combination from right and left side of the aircraft (67005/1 and 67009/7).
The controllers A 1.3 and A 1.4 were suboptimal controllers without observers.
Fig. 4.2-1 shows the principle signal flow within the black box for controller A 1.4 and its roll-off filter. For the controller A 1.3 there was no second high pass with the corner frequency of 1.5 Hz while controller A 2.8 had no digital filter at all but used an observer of reduced order (4 states to be compared with 32 states of the mathematical model of the aircraft) and no pseudo integration of measured accelerations.
For each controller design, all transfer functions of all related filters and of all degradations due to sampling rate of output (4ms) and pseudo-integration (T = 2 sec) were combined together and then approximated by polynomials. After that the resulting differential equations were coupled with the equations of the aircraft. This yielded the final equations of the plant to be controlled.
Application of optimal control theory as described in chapter 2 with different weighting matrices of states did not produce satisfactory results. Therefore arbitrary negative structural damping (1.4%) of the engine pitch mode was introduced into the flutter calculation. This resulted in a theoretical flutter instability with its minimum at 472 kts VCAS.
The optimal control theory was then applied again for the conditions of this velocity but without any weighting of states. This gave reasonable controllers. Fig. 4.2-2 shows the modal dampings of the aircraft with controller A 1.4 to be compared with Fig. 4.1-2. The frequencies are nearly unchanged and the same is approximately valid for the dampings with the exception of the damping belonging to the critical mode. Its dip disappeared completely. It has been turned into a strong maximum as is typical for optimal control theory.
The other controllers produced about the same result.

Before installation into the aircraft the controllers have been compared in the lab with real flight test data as input signals taken from a magnetic tape. The data were measured during excitation of the aircraft by the tip vane moving with a frequency sweep.
Fig. 4.2-3 shows the results. Time histories of controller output signals are plotted.
Heavy superimposed low frequency disturbances are seen in the signal of controller A 1.3 which was no longer tested due to this disadvantage.
Furthermore it is obvious that controller A 2.8 produces much smaller output signals and that means much smaller control surface movement which should be an advantage.

### 4.3 Results

#### 4.3.1 Comparison of Predicted and Measured Transfer Functions

First Fig. 4.3.1-1 shows the magnitude of the

predicted and the measured transfer function from tip vane movement to its lift force. The accuracy is rather good. The prediction has been made with the double lattice method (unmodified NASTRAN), but one should bear in mind that the tip vane is not a typical control surface installed in the down-wash of the wing.
It is also interesting to see that the total vertical load acting on the whole aircraft due to the movement of the tip vane is about twice as big as its lift force on the tip vane itself.

Next the transfer functions of the aircraft (in open loop) from actuator signal to vertical acceleration at wing tip (for both sides of the aircraft) are given in Fig. 4.3.1-2. Here the similarity is obvious but the accuracy is not as good as would perhaps be desirable.
(Besides, it must be said that the predicted curves are real predictions unmodified and without corrections for better matching with the measurements.)

### 4.3.2 Remarks about Lag-state Approximation

It may now be worthwile to come back to the mathematical model used for the unsteady aerodynamics. If a lag-state approximation is used instead of the method of modal synthesis, the computed transfer functions just discussed look a bit different as shown in Fig. 4.3.2-1. The tapered peak at 3.3 Hz is even higher and the differences to the test results are larger. This happens although the approximation of the airloads itself was rather good.

### 4.3.3 Efficiency of the Controllers

The final efficiency of the controllers A 1.4 and A 2.8 is clearly visible in Fig. 4.3.3-1 where the measured transfer functions from actuator signal to acceleration at wing tip and engine are shown in open and closed loop condition. The difference is large and could not be better. Especially the tapered peak of the flutter critical mode with about 3.3 Hz disappeared when the controllers were active.
This indicates that the aim has been reached and that the vibration amplitudes of wing tip and engine are reduced by the controller.

A comparison of controllers A 1.4 and 2.8 shows that controller A 1.4 is perhaps slightly more effective which may have been expected because its gain was a bit larger.

Modal analysis of the transfer functions shown in Fig. 4.3.3-1 yielded modal data. The modal damping found is marked in Fig. 4.3.3-2 together with the predictions taken from Fig. 4.2-2. The increase due to the controller is about 80%. Again the success is visible. The controller functioned as expected, it cured the artificially installed critical vibration.

## 5. Conclusions

Application of the vibration control technology to wind tunnel model and real aircraft under different conditions showed this technology to be an effective tool for flutter suppression (or margin augmentation) and amplitude smoothing with inherent load alleviation capacity. This means an additional tool is available for application even on civil aircraft.
Know-how has been acquired.

## References


1. Kwakernaak, H. Sivan, R.
   "Linear Optimal Control Systems"
   John Wiley & Sons Inc. New York 1972

2. Mukhopadhyay, J.R; Newson, J.R; Abel, I.
   "A Method for Obtaining Reduced-Order Control Laws for High-Order Systems Using Optimisation Techniques"
   NASA TP 1876, 1981

3. Försching, H. (editor)
   "Active Control Application for Flutter Suppression and Gust Load Alleviation, Results of Phase 1 to 3".
   GARTEUR TP-022, 1985.

4. König, K.
   "Experience from Flight Flutter Testing with Tip Vanes on Airbus" DGLR Bericht 82-1, International Symposium on Aeroelasticity Nuremberg/W.Germany Oct. 5-7, 1981.


system:

$$MS \cdot \ddot{qS} + DS \cdot \dot{qS} + KS \cdot qS + pL = \Phi H' \cdot pH \qquad 2.1\text{-}1$$

airloads:

$$pL \approx ML \cdot \ddot{qS} + DL \cdot \dot{qS} + KL \cdot qS \qquad 2.1\text{-}2$$

combined:

$$\begin{bmatrix} \dot{qS} \\ \ddot{qS} \end{bmatrix} = \begin{bmatrix} 0 & 1 \\ -(MS+ML)^{-1} \cdot (KS+KL) & -(MS+ML)^{-1} \cdot (DS+DL) \end{bmatrix} \cdot \begin{bmatrix} qS \\ \dot{qS} \end{bmatrix} + \begin{bmatrix} 0 \\ (MS+ML)^{-1} \cdot \Phi H' \end{bmatrix} \cdot qH \qquad 2.1\text{-}3$$

eigenvalue solution:

$$\begin{bmatrix} 0 & 1 \\ -(MS+ML)^{-1} \cdot (KS+KL) & -(MS+ML)^{-1} \cdot (DS+DL) \end{bmatrix} = \begin{bmatrix} \Phi F & \Phi F^* \\ \Phi F \cdot \lambda F & \Phi F^* \cdot \lambda F^* \end{bmatrix} \cdot \begin{bmatrix} \lambda F & 0 \\ 0 & \lambda F^* \end{bmatrix} \cdot \begin{bmatrix} \Phi F & \Phi F^* \\ \Phi F \cdot \lambda F & \Phi F^* \cdot \lambda F^* \end{bmatrix}^{-1} \qquad 2.1\text{-}4$$

state equation:

$$\begin{bmatrix} \dot{qS} \\ \ddot{qS} \end{bmatrix} = \begin{bmatrix} \Phi F & \Phi F^* \\ \Phi F \cdot \lambda F & \Phi F^* \cdot \lambda^* \end{bmatrix} \cdot \begin{bmatrix} \lambda F & 0 \\ 0 & \lambda F^* \end{bmatrix} \cdot \begin{bmatrix} \Phi F & \Phi F^* \\ \Phi F \cdot \lambda F & \Phi F^* \cdot \lambda F^* \end{bmatrix} \cdot \begin{bmatrix} qS \\ \dot{qS} \end{bmatrix} + \begin{bmatrix} 0 \\ MS^{-1} \cdot \Phi H' \end{bmatrix} qH \qquad 2.1\text{-}5$$

abbreviated:

$$\dot{x} = A \cdot x + B \cdot u \qquad 2.1\text{-}6$$

**Fig. 2.1-1: STATE-EQUATIONS FROM MODAL SYNTHESIS**

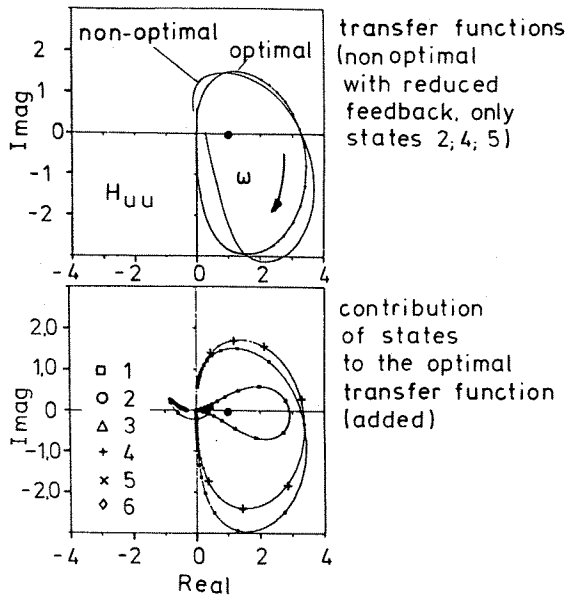


**Fig. 2.2-1: NON-OPTIMAL APPROXIMATION OF CONTROLLER**

equation available (aircraft):

$\dot{x}_1 = A_1 \cdot x_1 + B_1 \cdot u_1$

$y_1 = C_1 \cdot x_1$

transfer function measured (actuator):

$H_{x2,u2}(\omega)$

polynomial approximation:

$$Min = \sum_{\omega} \left(H_{x2,u2}(\omega) - \frac{\sum_n an \cdot (i\omega)^n}{\sum_m bm \cdot (i\omega)^m}\right)^2$$

partial fractions:

$$\frac{\sum_n an \cdot (i\omega)^n}{\sum_m bm\,(i\omega)^m} = \sum_e \frac{re}{i\omega - \lambda e}$$

state equation:

$\dot{x}_2 = [\lambda e] \cdot x_2 + [1] \cdot u_2$

$y_2 = [re] \cdot x_2$

plant:

by coupling ($y_2 = u_{12}$)

$$\begin{bmatrix} \dot{x}_1 \\ \dot{x}_2 \end{bmatrix} = \begin{bmatrix} A_1 & B_{12} \cdot [re] \\ 0 & [\lambda e] \end{bmatrix} \cdot \begin{bmatrix} x_1 \\ x_2 \end{bmatrix} + \begin{bmatrix} B_{11} & 0 \\ 0 & [1] \end{bmatrix} \cdot \begin{bmatrix} u_{11} \\ u_2 \end{bmatrix}$$

$$\begin{bmatrix} y_1 \\ y_2 \end{bmatrix} \quad \begin{bmatrix} C_1 & 0 \\ 0 & re \end{bmatrix} \begin{bmatrix} x_1 \\ x_2 \end{bmatrix}$$

optimal control theory:

$$Min = \int_0^{\infty} (x' \cdot QX \cdot x + u' \cdot QU \cdot u) \cdot dt$$

$u = -KX \cdot x$ ; KX from $\begin{bmatrix} A & -B \cdot QU^{-1} \cdot B' \\ -QX & -A' \end{bmatrix}$

$H_{u,u}(\omega) = -KX \cdot ([i\omega] - A)^{-1} \cdot B$

suboptimal approximation:

$$Min = \sum_{\omega} ((KY \cdot C - KX) \cdot ([i\omega] - A)^{-1} \cdot B)^2$$

$u = -KY \cdot y$ controller

**Fig. 2.2-2: PRINCIPLES OF SUBOPTIMAL CONTROLLER DESIGN**

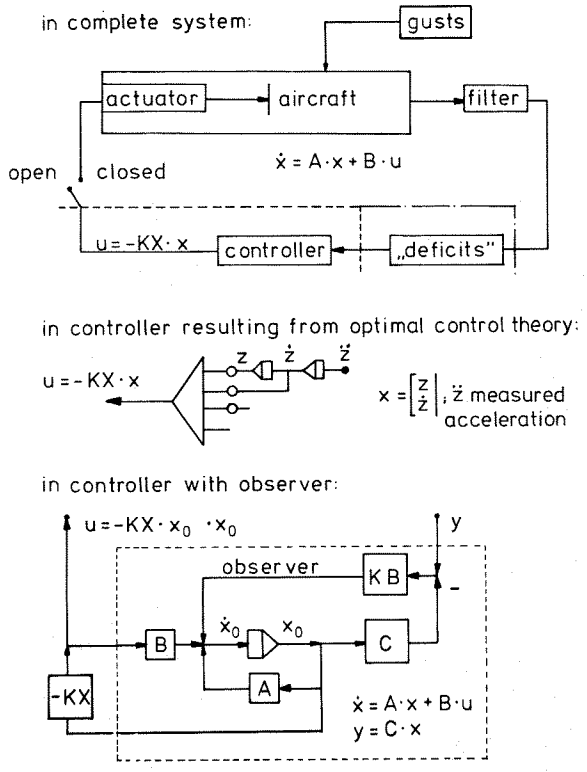


**Fig. 2.3-1: PRINCIPLE SIGNAL FLOW**

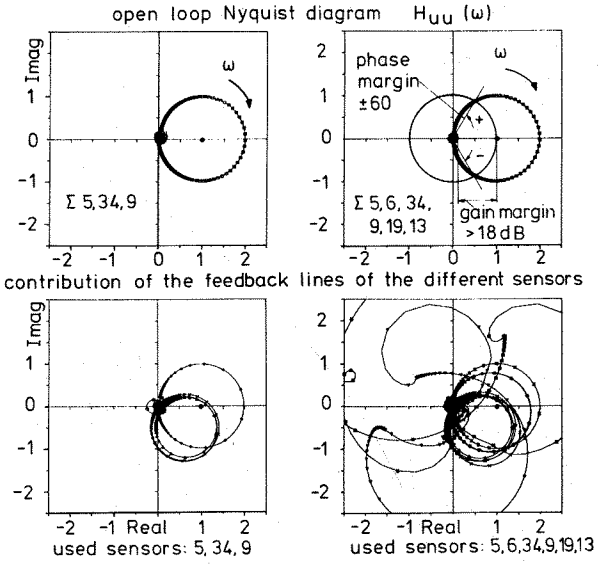


**Fig. 2.5-1: INFLUENCE OF SENSOR LOCATION ON SUBOPTIMAL CONTROLLERS**

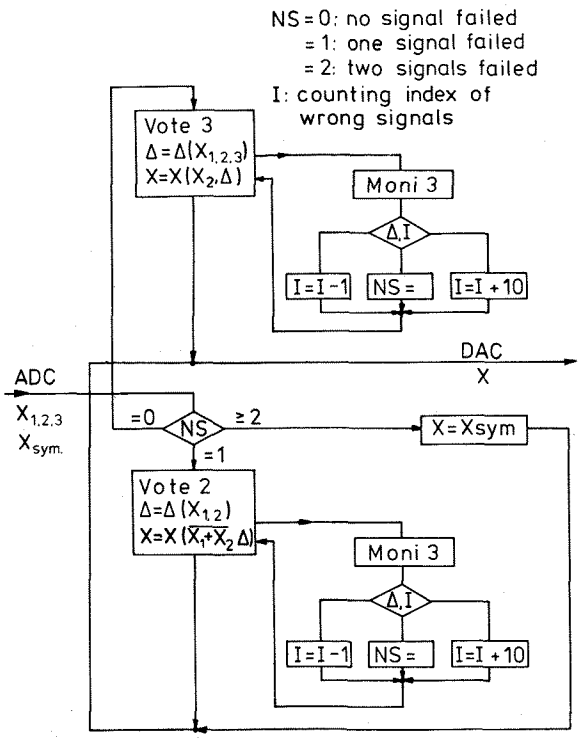


**Fig. 2.6-1: SIGNAL CONDITIONER**

| controller No. | name | surface sensors used: analog/digital | taileron/aileron/spoiler | No. of accelerometer | | design: suboptimal controller | r: rigid body stability f: flutter speed increase g: gust load alleviation | observer | pseudo integration | filter | No. of combined taileron controller | result: max. wind vel. reached |
|---|---|---|---|---|---|---|---|---|---|---|---|---|
| 1 | G6.1 | D | tail | | ϑ̇ | X | r | 0 | X | L1 | / | / |
| 2 | G7.1 | D | tail | | ϑ̇ | X | r | 0 | X | L1 | / | / |
| 3 | LKE | A | tail | | ϑ̇ | 0 | r | 0 | X | L1 | / | / |
| 4 | G2.3 | A | ail | 2/14 | 3/19 | X | f+g | 0 | X | B1 | 3 | 54 |
| 5 | G2.3 | D | ail | 2/14 | 3/19 | X | f+g | 0 | X | B2* | 3 | 54 |
| 6 | G2.3 | A** | sp. | 2/14 | 3/19 | X | f+g | 0 | X | B1 | 3 | 53 |
| 7 | G2.2 | A | ail | 2/14 | 3/19 | X | f | 0 | X | B1 | 3 | 56 |
| 8 | G2.2 | A | ail | 2/ | 3/ | X | f | 0 | X | B1 | 3 | 55 |
| 9 | G2.2 | A | ail | /14 | /19 | X | f | 0 | X | B1 | 3 | 55 |
| 10 | G3.1 | A | ail | 5/15 | 1/13 | X | f | 0 | X | B1 | 1,3 | 57 |
| 11 | G3.1 | D1 | ail | 5/15 | 1/13 | X | f | 0 | X | B2* | 3 | 57 |
| 12 | G3.1 | D2 | ail | 5/15 | 1/13 | X | f | 0 | X | B3* | 1-3 | 57 |
| 13 | G3.5 | D | ail | 5/15 | 1/13 | X | f | 0 | X | B3 | 1 | 57 |
| 14 | G4.1 | D | ail | / | 1/13 | 0 | f | X | X | B3 | 1 | 53 |
| 15 | G4.2 | D | ail | / | 1/13 | 0 | f | X | 0 | B4 | 1,2 | 52 |
| 16 | G3.1 | A | ail | 5/15 | / | X | f | 0 | X | B1 | 3 | 52 |
| 17 | G3.1 | A | ail | / | 1/13 | X | f | 0 | X | B1 | 3 | 47 |
| 18 | G3.1 | A** | sp. | 5/15 | 1/13 | X | f | 0 | X | B1 | 3 | 51 |

**Fig. 3.2-1: TESTED CONTROLLERS**

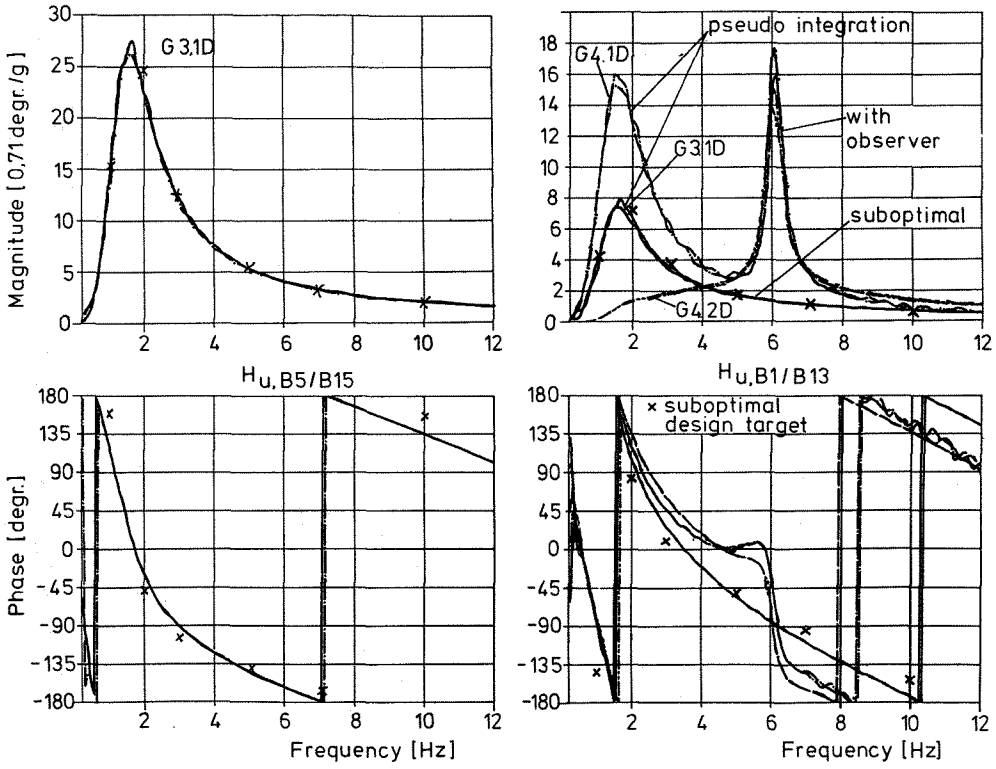


**Fig. 3.2-2: TRANSFER FUNCTIONS OF CONTROLLERS G3.1D; G4.1D; G4.2D (Including filters)**

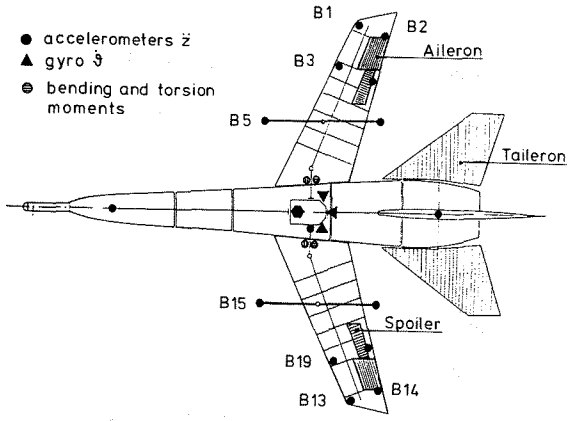


**Fig. 3.1-1: SENSOR INSTALLATION**

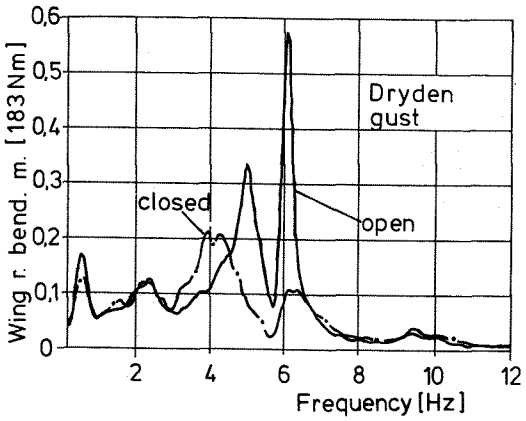


**Fig. 3.3.2-1: LOAD ALLEVIATION BY CONTROLLERS (G2.3A; 35m/s)**

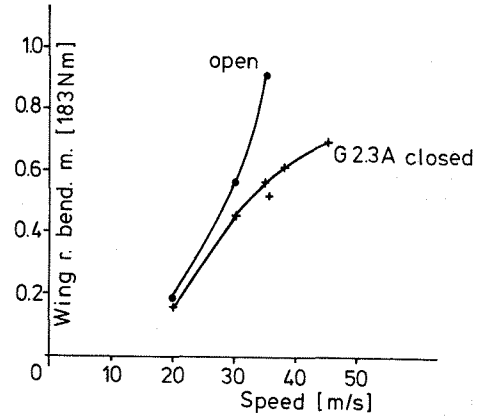


**Fig. 3.3.2-2: INFLUENCE OF SPEED ON LOAD ALLEVIATION (Dryden gust) (rms values in frequency band 2.5-6.5Hz)**

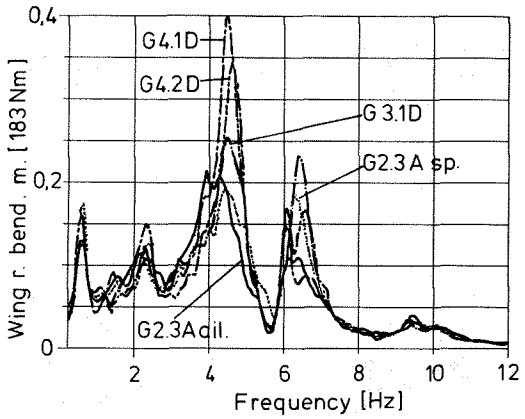


**Fig. 3.3.2-3: INFLUENCE OF CONTROLLER ON WING ROOT BENDING MOMENT (35m/s; (Dryden gust)**

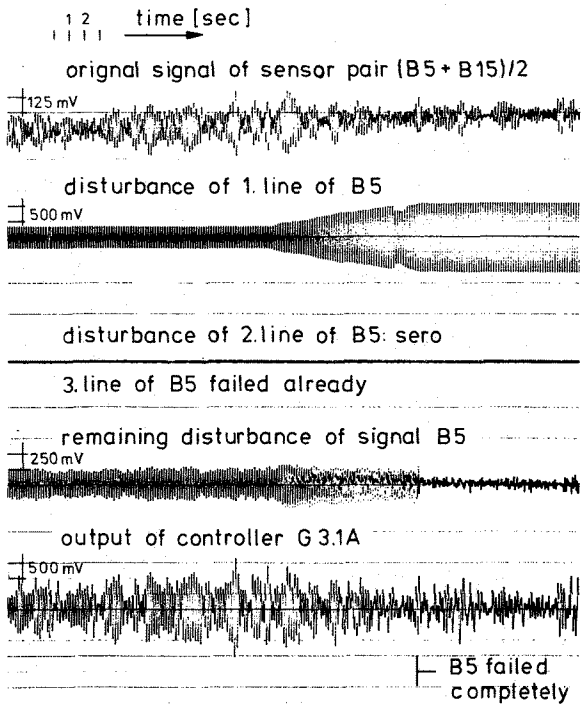


**Fig. 3.3.3-1: INFLUENCE OF SIGNAL CONDITIONING (45m/s)**

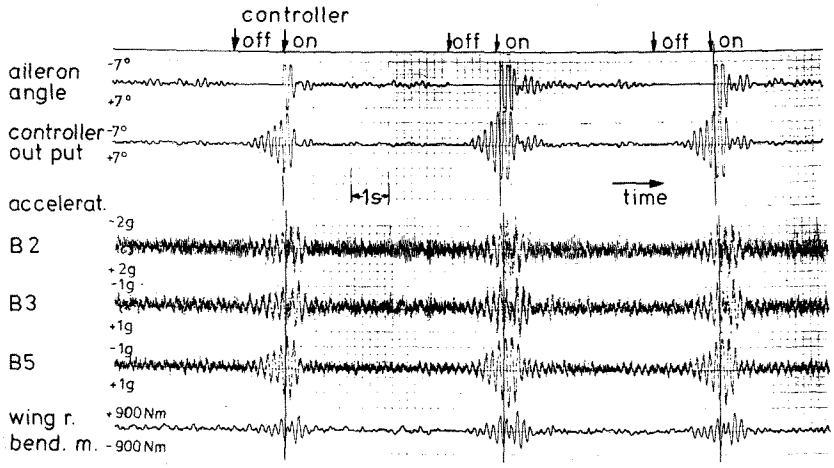


**Fig. 3.3.3-2: LOSS OF CONTROLLER IN FLIGHT (52m/s; G3.1A)**

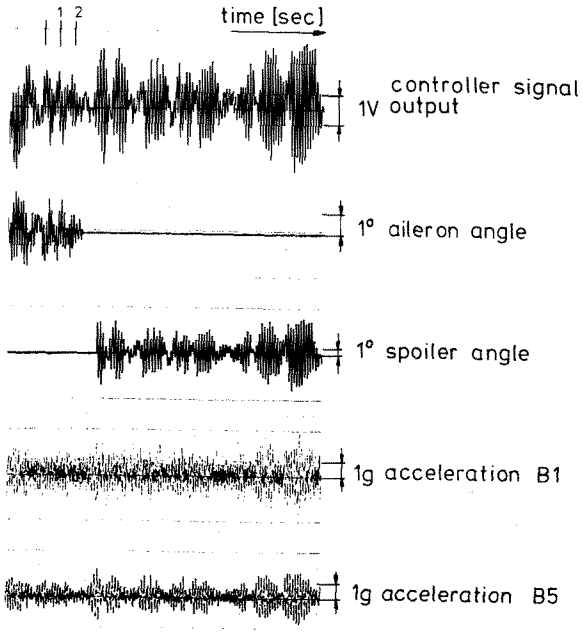


**Fig. 3.3.3-3: EXCHANGE OF CONTROL SURFACE IN FLIGHT (45m/s; D. g.; G3.1A)**

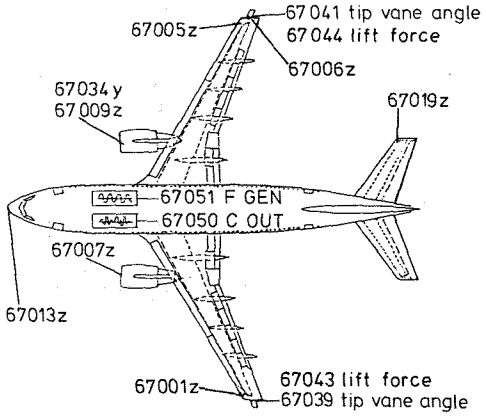


**Fig. 4.1-1: POSITION OF RELEVANT SENSORS AT A310-300**

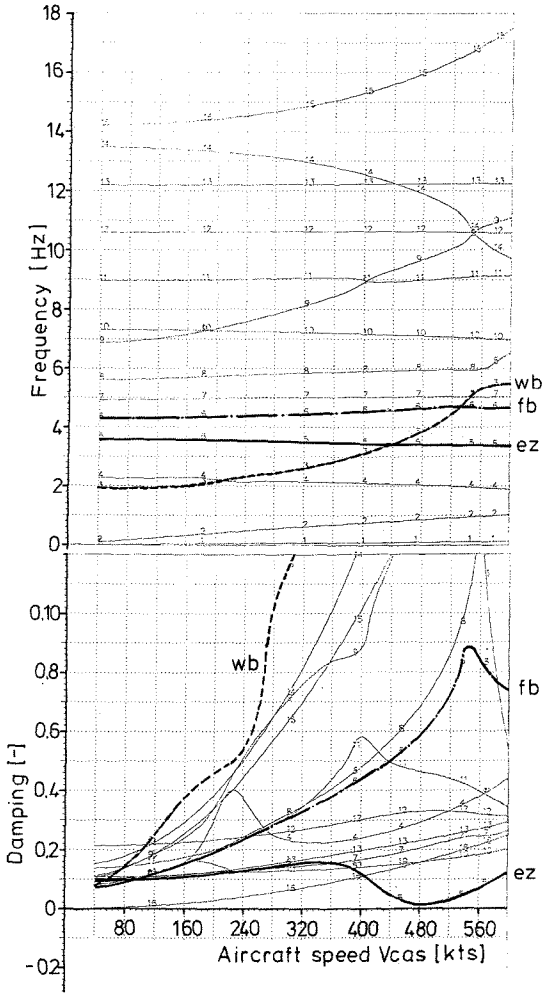


**Fig. 4.1-2: EIGENVALUES WITHOUT CONTROLLER**

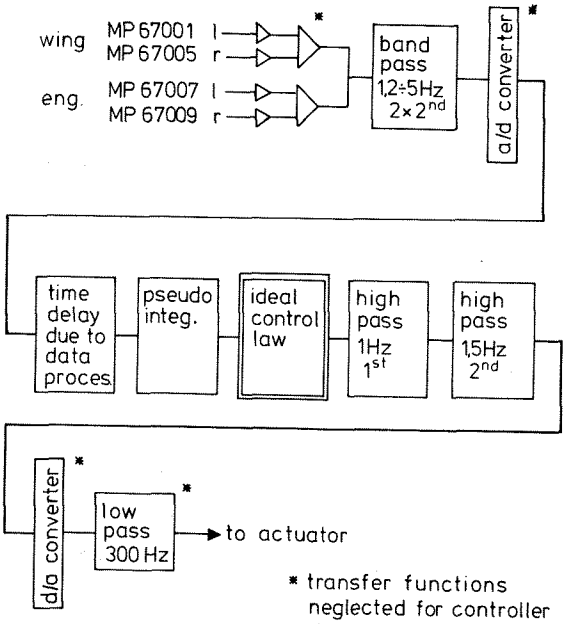


**Fig. 4.2-1: SIGNAL FLOW IN CONTROLLER A 1.4**

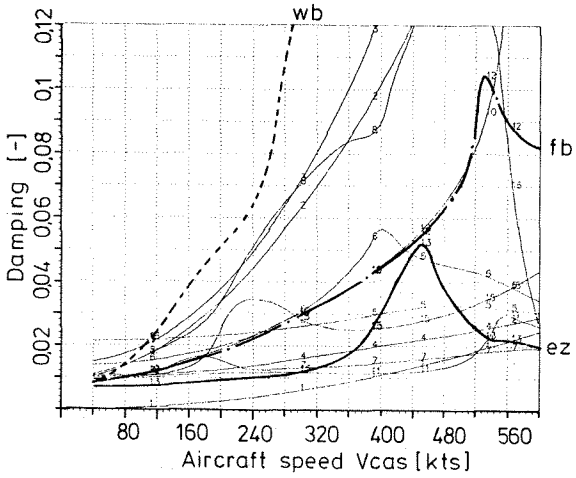


**Fig. 4.2-2: MODAL DAMPING WITH CONTROLLER**

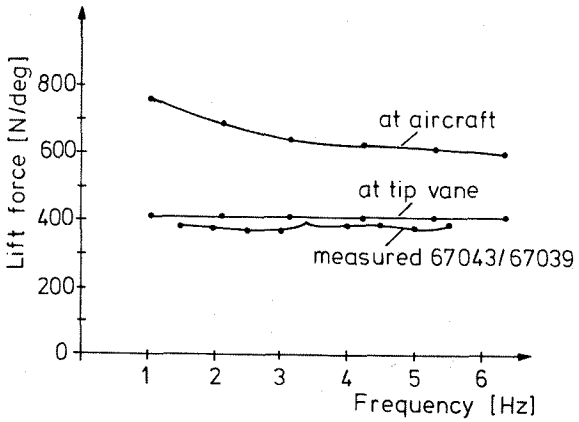


**Fig. 4.3.1-1: LIFT FORCE DUE TO TIP VANE MOVEMENT (400KCAS, 0.84MA)**

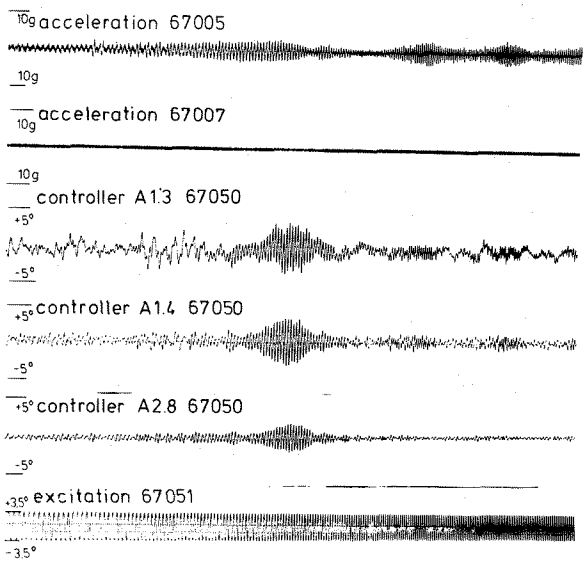


**Fig. 4.2-3: OUTPUT OF CONTROLLERS (400KCAS; 0,84MA; open loop; sweep: 3,5°; 1.4-5.6Hz; 30 sec/oct.)**

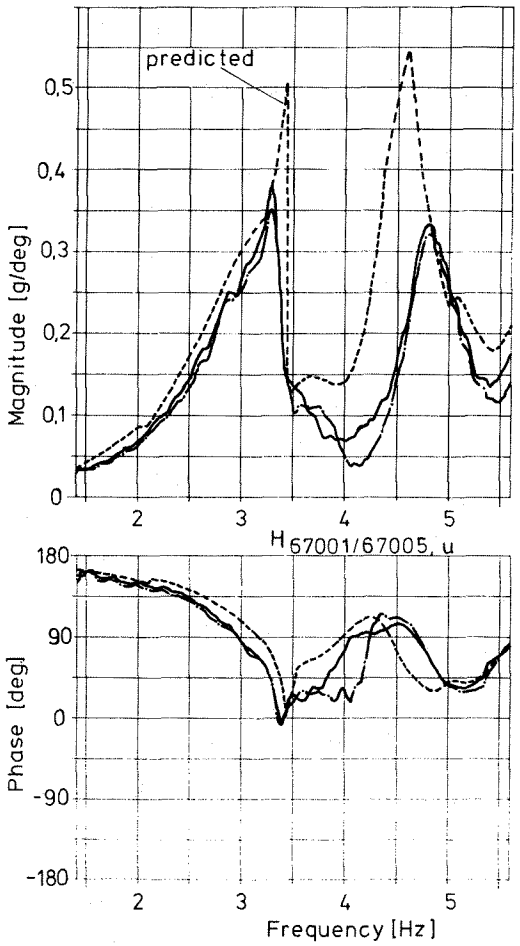


**Fig. 4.3.1-2: TRANSFER FUNCTIONS OF PLANT (400KCAS; 0.84 MA)**

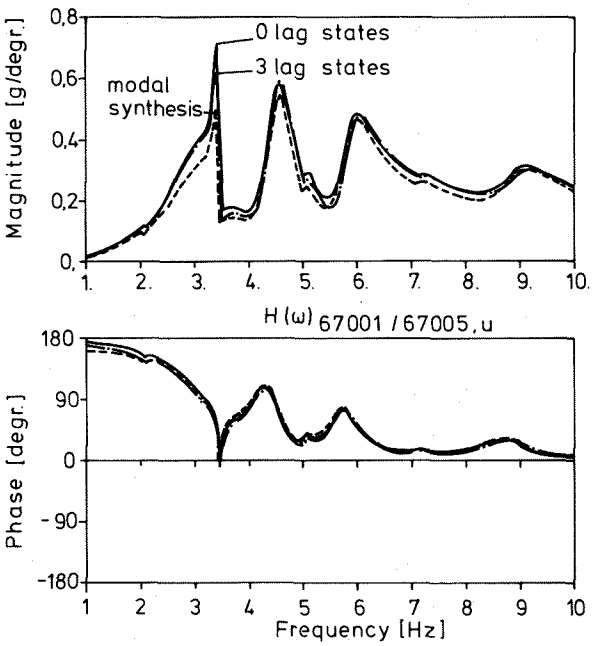


**Fig. 4.3.2-1: INFLUENCE OF UNSTEADY AERODYNAMIC APPROXIMATION ON TRANSFER FUNCTION OF PLANT (400KCAS; 0.84 MA)**

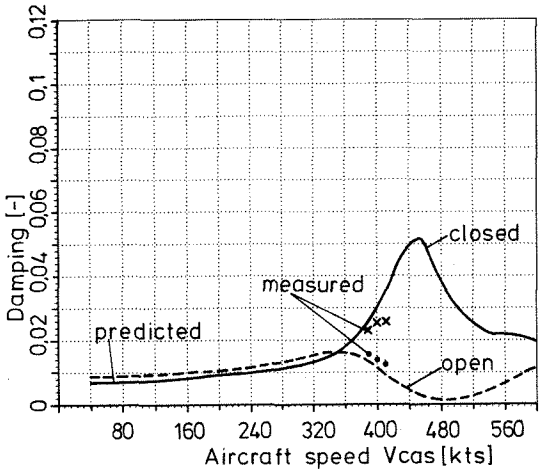


**Fig. 4.3.3-2: MODAL DAMPING WITH AND WITHOUT CONTROLLER A1.4**

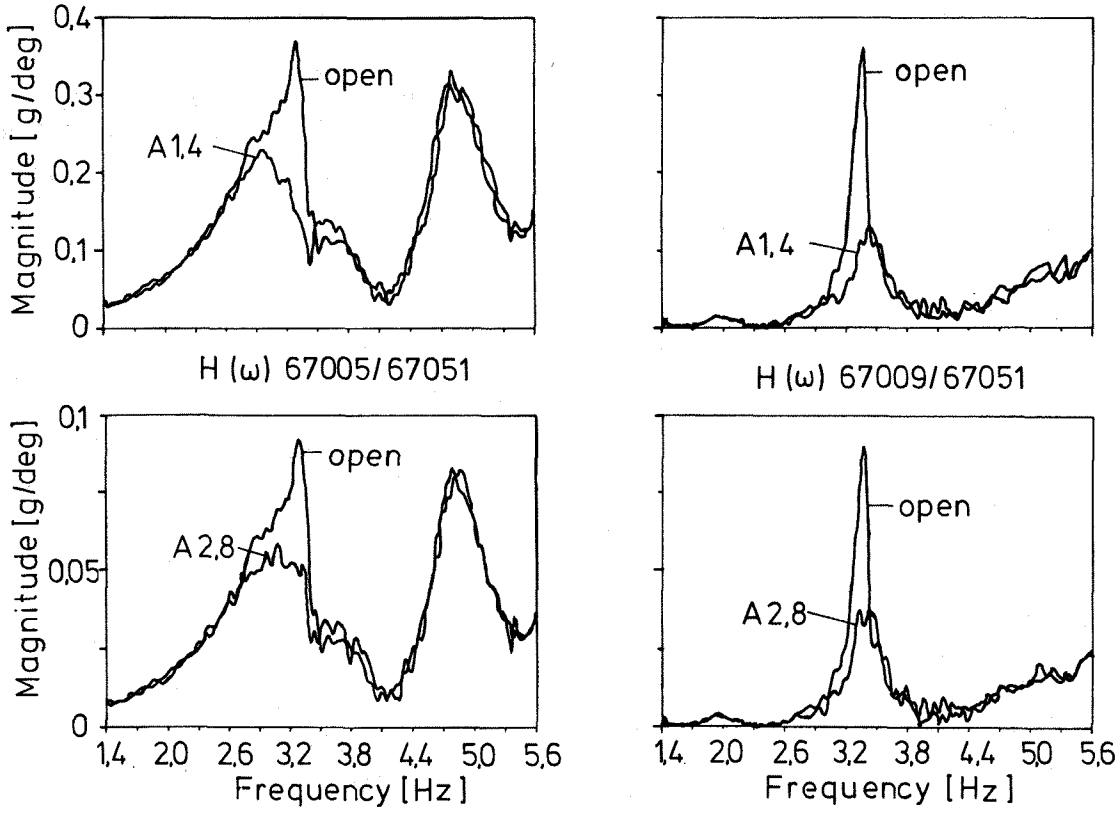


**Fig. 4.3.3-1: EFFICIENCY OF CONTROLLERS (400KCAS; 0.84 MA)**